Kinetik: Game Technology, Information System, Computer Network, Computing, Electronics, and Control
Journal homepage: http://kinetik.umm.ac.id
ISSN: 2503-2267
Vol. 11, No. 2, May, Pp. 285-294

Identification of BSR disease in oil palm using UAV imagery through CNN and SCNN approaches

Zakia Azzahro[1], Rahmadwati*[1], Angger Abdul Razak[1], Amrul Faruq[2]
Electrical Engineering Department, Universitas Brawijaya, Malang, Indonesia[1]
Electrical Engineering Department, Faculty of Engineering, Universitas Muhammadiyah Malang, Indonesia[2]

Article Info
Keywords:
Basal Steam Roat, Palm Oil, Deep Learning, UAV Imagery, CNN, SCNN

Article history:
Received: October 25, 2025
Accepted: December 25, 2025
Published: May 01, 2026

Cite:
Z. Azzahro, Rahmadwati, Angger Abdul Razak, and Amrul Faruq, "Identification of BSR Disease in Oil Palm Using UAV Imagery through CNN and SCNN Approaches", *KINETIK*, vol. 11, no. 2, May 2026.
https://doi.org/10.22219/kinetik.v11i2.2546

*Corresponding author.
Rahmadwati
E-mail address:
rahma@ub.ac.id

Abstract
Basal Stem Rot (BSR) disease caused by Ganoderma boninense is a major threat to oil palm productivity due to its destructive nature and the challenges associated with early-stage detection. To support sustainable production and mitigate significant yield losses, a system capable of classifying oil palm trees into healthy and infected categories is required. In this study, two deep learning approaches, namely CNN and SCNN, are applied to identify oil palm conditions based on UAV-derived imagery. While CNN is widely used for image-based detection tasks due to its capability to extract relevant visual representations, it is prone to overfitting during training. Therefore, SCNN is employed to address this issue by leveraging image similarity comparison mechanisms. Experimental results show that both methods achieve high classification accuracy, with SCNN outperforming CNN by achieving an accuracy of 96.48% compared to 95.644% for CNN. The superior performance of SCNN indicates its sensitivity to subtle visual differences between healthy and early-stage infected oil palm trees, enabling more reliable classification performance. Thus, SCNN is considered more effective for oil palm condition detection and contributes to reducing overfitting, resulting in improved model stability.

1. Introduction

Oil palm is a leading commodity in the agribusiness sector of Southeast Asia, particularly in Indonesia and Malaysia, playing a strategic role in the national economy as a source of income and employment [1]. The global palm oil industry holds substantial economic value, reaching USD 65.73 billion in 2015 and continuing to expand. Indonesia and Malaysia contribute approximately 85% of the world's palm oil supply, making production sustainability crucial for maintaining global market stability [2], [3]. However, since 2009, Indonesia's palm oil production has declined due to infectious diseases, causing yield losses of up to 80% [4]. Basal Stem Rot (BSR), caused by the pathogenic fungus *Ganoderma boninense*, is recognized as one of the most detrimental diseases affecting oil palm plantations because of its highly infectious nature and rapid transmission through root contact and soil-based inoculum. This disease has caused major economic losses estimated at USD 50–350 million [5]. Traditional disease identification approaches predominantly rely on manual field inspections, which are time-consuming, labor-intensive, and less suitable for large-scale plantation areas, particularly during early infection stages where visual symptoms are minimal and can easily be mistaken for healthy plant characteristics. Consequently, advancements in digital image processing and machine learning have increasingly been explored as promising alternatives for early and non-invasive disease detection, offering improved accuracy, efficiency, and scalability in monitoring oil palm plantation health without requiring continuous field-based inspection [2], [4], [6].

Satelite and UAV imagery have been widely used for large-scale plantation monitoring [7]. However, UAV imagery offers superior spatial resolution and operational flexibility because UAVs can operate at lower altitudes and capture high-resolution, up-to-date images. In contrast, satellite imagery covers larger geographical areas at lower operational cost but suffers from lower spatial resolution and susceptibility to atmospheric disturbances. Therefore, UAV imagery is considered more suitable for detailed plantation monitoring due to its higher spatial resolution and greater operational flexibility [3], [8]. Nevertheless, despite these advantages, detecting BSR disease in oil palm plantations remains challenging because early-stage symptoms often resemble healthy plants, while high canopy density causes crown overlap, reducing object visibility and classification accuracy, particularly in large-scale plantations.

Several previous studies have attempted to address the challenges associated with detecting BSR disease in oil palm plantations. Research employing the YOLOv5 method demonstrated the capability to classify oil palm tree conditions with an average F1-score of 0.878 and precision exceeding 0.961 across all classes. However, the model performed less effectively on minority classes and was not specifically optimized for early-stage disease detection [9]. Another study employed the M-CR U-Net method, achieving an F1-score of 0.978 and precision of 0.986. Nevertheless,

reliance solely on RGB imagery limits the accuracy of early disease detection, particularly during the initial stages of infection [4].

This study aims to improve the detection capability of BSR disease in oil palm trees through the implementation of CNN and SCNN approaches. Previous research has shown that CNNs provide strong classification performance, while SCNN approaches are effective in mitigating overfitting problems [10], [11]. Convolutional Neural Network (CNN) are among the most widely used deep learning methods and have become well-established architectures in the development of image-processing models. The primary advantage of CNNs over conventional approaches lies in their capability to automatically extract discriminative features directly from input data, enabling an integrated and structured process of feature extraction and classification [12]. Meanwhile, the Siamese Convolutional Neural Network (SCNN) approach is employed to compare feature representations between image pairs more effectively and has been shown to mitigate overfitting problems [11].

2. Research Method

This research applies deep learning techniques based on CNN and SCNN models to detect the presence of BSR disease in oil palm trees. The proposed workflow consists of three main stages: image data acquisition, data pre-processing to improve data quality, and model training and evaluation. The system ultimately produces detection results that distinguish between healthy oil palm trees and those infected with BSR disease.

2.1 Data Preprocessing

The initial stage of this research involves data pre-processing. The data utilized in this study consist of oil palm images acquired using an Unmanned Aerial Vehicle (UAV). The use of UAVs enables the efficient acquisition of high-resolution aerial imagery over large plantation areas that are difficult to access manually. The dataset employed in this research was obtained from the Kaggle platform (www.kaggle.com), which contains a collection of oil palm images with a resolution of 1024 × 1024 pixels [8].

The data pre-processing stage begins with the bounding box annotation process, which is performed to label specific regions within the images representing healthy and BSR-infected oil palm trees. This process enables the model to recognize and focus on relevant regions of interest associated with disease detection. Sample images annotated using bounding boxes are presented in Figure 1.

Figure 1. Dataset Samples Annotated with Bounding Boxes

Subsequently, an image extraction process is conducted, in which the plant regions identified by the bounding boxes are systematically cropped from the original images and stored in separate directories according to their respective categories, namely healthy and infected oil palm trees. This step ensures that only relevant regions of interest are utilized for subsequent analysis, thereby reducing background noise and improving detection reliability. The dataset employed in this study consists of a total of 2,600 oil palm tree images, including both healthy and BSR-infected samples. To support effective model training and evaluation, the dataset is divided into training and validation subsets, with 70% of the images allocated for training and the remaining 30% reserved for validation. This data partitioning strategy is intended to facilitate robust model learning while providing an unbiased evaluation of model performance on previously unseen data.

Following dataset partitioning, an image augmentation stage is applied to improve both the quality and diversity of the training data. Augmentation is performed to address potential data imbalance and enhance model generalization by exposing the network to a wider range of visual variations. In this study, contrast enhancement is employed as the primary augmentation technique because it effectively highlights subtle visual patterns associated with early-stage BSR symptoms in oil palm trees, including changes in color and texture. By improving the visibility of these discriminative

features, the augmentation process contributes to more reliable feature extraction and disease detection performance. The distribution of healthy and diseased oil palm tree samples used in this study is presented in Table 1 [4].

Table 1. Examples of Expert-annotated Images Along with Descriptions of Each Image

Dataset Sample	Classification	Description
	Healthy	A healthy oil palm tree generally exhibits a canopy with uniformly bright green coloration across the leaf surfaces, along with dense and lush foliage, indicating optimal growth condition.
	BSR-infected	Oil palm trees exhibiting canopy wilting generally experience a decline in overall plant vitality, which is characterized by reduced leaf density and a smaller, less uniform canopy structure. This condition often reflects physiological stress caused by disturbances in water and nutrient transport and may serve as an important visual indicator of underlying plant health problems.
	BSR-infected	Oil palm leaves exhibit increased intensity and broader distribution of yellow spots, indicating physiological stress and pigmentation changes that can serve as visual indicators of declining plant health.
	BSR-infected	Oil palm trees experiencing health decline often exhibit grayish coloration accompanied by wilted and dried canopies.

2.3 Convolutional Neural Network (CNN)

CNNs are a class of deep learning models specifically designed to effectively process two-dimensional (2D) data formats, such as visual images or acoustic signals [13]. CNNs operate under a supervised learning framework, where the model is trained using labeled data with predefined target variables, enabling it to classify new data based on previously learned patterns. CNNs are widely applied in various image processing tasks, including object recognition, scene recognition, object detection, segmentation, and image classification [14].

In CNN architectures, each input image undergoes successive processing stages beginning with convolutional and pooling layers to extract hierarchical features progressively. Subsequently, the resulting feature maps are reshaped into a flattened vector and processed through fully connected layers to determine the final class output [15], [16]. The overall architecture of the CNN process is illustrated in Figure 2.

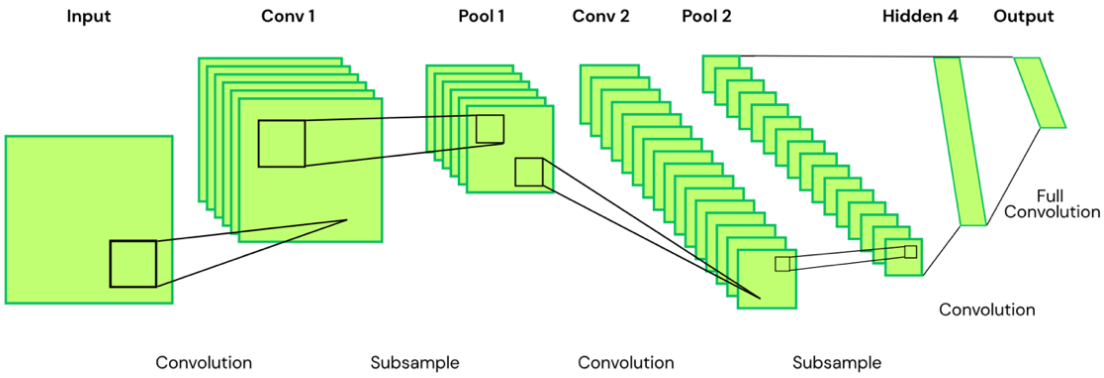

Figure 2. Archirecture of Convolutional Neural Network

Figure 2 presents the fundamental structure of a CNN, which consists of multiple processing components [17]. The network begins with an input layer responsible for receiving image data, followed by a sequence of convolutional layers that extract important visual features and pooling layers that reduce data dimensionality while preserving essential information. The resulting feature maps are subsequently flattened and passed through fully connected (hidden) layers, where the extracted representations are combined and refined. Finally, the output layer generates the predicted class label. This architecture illustrates how CNNs progressively build feature representations from low-level features, such as edges and textures, to high-level abstract patterns, enabling effective identification of complex visual characteristics [10], [18], [19].

2.4 Siamese Convolutional Neural Network (SCNN)

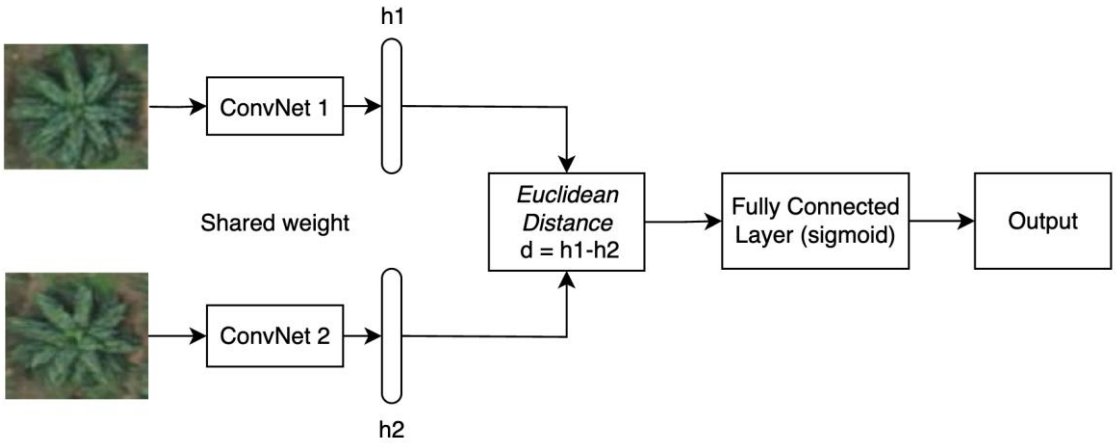

Figure 3. Architecture of SCNN

Figure 3 illustrates the architecture of the SCNN [11], which is an artificial neural network designed to compare or match two input images. The architecture consists of two identical CNN branches, each receiving different inputs but connected through a shared output layer [20]. The system processes image pairs, where one of the images is labeled, to learn a similarity metric by training both CNN branches using identical weights. Each CNN independently processes its respective input and generates feature representations. These feature representations are subsequently combined and processed by the output layer to produce a similarity score indicating the degree of resemblance between the two inputs [21].

The output of the SCNN is represented as a binary value, where $EW = 0$ indicates that the image pair belongs to different categories, while $EW = 1$ denotes that both images belong to the same category. The weights in the SCNN are shared to map the patterns of the input pairs and extract key features, which are subsequently compared during the final stage of the process. To measure similarity, Euclidean Distance is employed to calculate the distance between the feature outputs generated by each CNN branch, as formulated in Equation 1[21].

$$d(x,y) = \sqrt{\sum_{i=1}^{n} (x_i - y_i)^2} \quad (1)$$

Where:
$d(x,y)$ = Euclidean distance betweenn two points *x* and *y*
n = Dimensions in the vector space
x_i = The coordinate of *x*
y_i = The coordinate of *y*
$(x_i - y_i)^2$ = The squared difference between the *i*-th coordinates of the two points

2.5 Model Training

The CNN and SCNN architectures were selected as the primary models in this study because both provide a favorable balance between detection accuracy and computational efficiency for identifying BSR disease in oil palm trees. The model training process was conducted using Visual Studio Code and the Python programming language. The learning rate and batch size were determined through an experimental hyperparameter tuning process and were applied consistently across both models. The detailed configuration of the training hyperparameters is presented in Table 2.

Table 2. CNN and SCNN Model Training Parameters

Parameters	Values
Model	CNN and SCNN
Epoch	100
Batch	32
Learning Rate	0.01
Optimizer	Adam

2.6 Performance Analysis

The analysis of experimental results was conducted to evaluate the performances of the developed models and to assess the extent to which the implemented methods achieved the research objectives. Furthermore, this stage aimed to obtain accurate and relevant data as the basis for comparative analysis in accordance with the objective of the study. The evaluation was performed using several performance metrics, including confusion matrix, accuracy, loss, precision, recall, and F1-score. These evaluation metrics serve as the primary indicators for assessing the effectiveness and performance of the proposed methods [22], [23].

Accuracy, as defined in Equation 2, measures the overall correctness of the model by comparing the number of correctly predicted instances (true positives and true negatives) to the total number of predictions. It is widely used as a general performance indicator, particularly when the dataset is relatively balanced [24], [25].

$$Acurracy = \frac{TP + TN}{TP + FN + FP + TN} \quad (2)$$

Precision, as shown in Equation 3, evaluates the proportion of correctly predicted positive observations relative to the total predicted positives. This metric is particularly important in cases where false positives must be minimized.

$$Precision = \frac{TP}{FP + TP} \quad (3)$$

Recall, presented in Equation 4, measures the model's ability to correctly identify all relevant instances and is calculated as the ratio of true positives to the sum of true positives and false negatives.

$$Recall = \frac{TP}{TP + FN} \quad (4)$$

F1-score, as expressed in Equation 5, represents the harmonic mean of precision and recall, providing a balanced evaluation metric when class distribution is uneven. This metric is especially useful when both false positives and false negatives are equally important to consider.

$$F1\ Score = \frac{2\ \times precision\ \times recall}{precision + recall} \quad (5)$$

Where:
TP = *True Positive*
TN = *True Negative*
FP = *False Positive*
FN = *False Negative*

3. Results and Discussion

This section presents the experimental results obtained using CNN and SCNN models for identifying BSR in oil palm trees. The results are analyzed from both quantitative and qualitative perspectives to evaluate model performance based on several metrics, including accuracy, precision, recall, and F1-score. In addition, a comparative analysis is presented to examine the extent to which the SCNN architecture improves early-stage BSR detection performance compared to the standard CNN model.

3.1 Convolutional Neural Network (CNN)

The training process of the CNN model was conducted with 100 epochs to detect BSR disease in oil palm trees based on the pre-processed image data and to determine the epoch that produced the best performances. The results indicate that the model achieved stable performance with a final loss value of 0.1876, a Mean Squared Error (MSE) of 0.4663, and an overall accuracy of 0.9564.

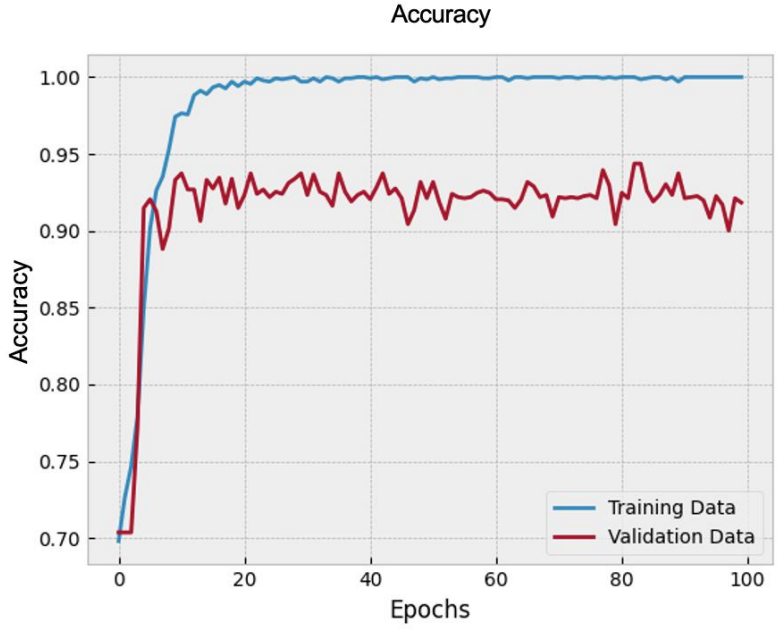

Figure 4. CNN Acurracy Graph

Figure 4 presents accuracy graph, which demonstrates a significant increase during the early phase of training and reaches a stable point after the 40th epoch. The training and validation accuracy curves exhibit a relatively balanced pattern, suggesting that the model did not experience significant overfitting. This stability indicates that the model effectively learned image feature across both the training and validation datasets.

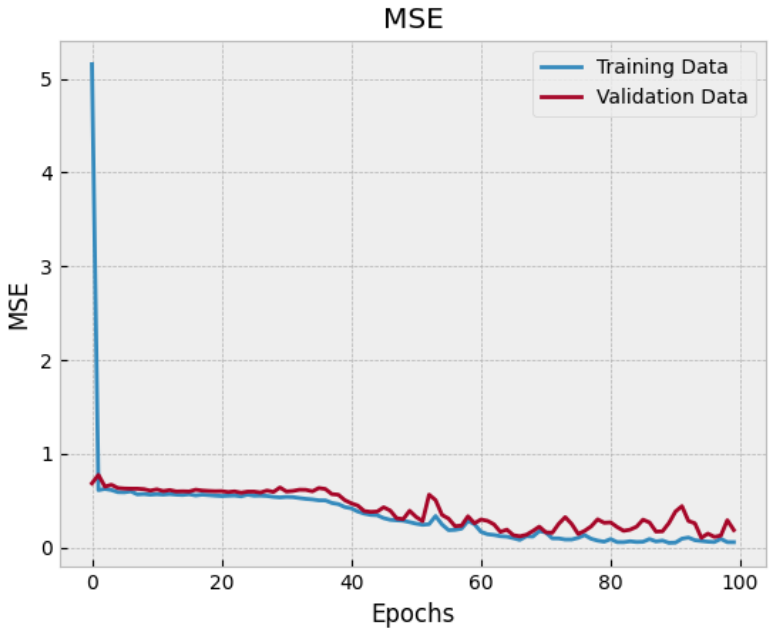

Figure 5. CNN MSE Graph

Figure 5 shows that the MSE value decreased sharply during the early stages of training and stabilized near zero after the 40th epoch. This trend confirms that the difference between the predicted and actual values became smaller as the number of training iterations increased, reflecting an improvement in the model's predictive performance on the validation data.

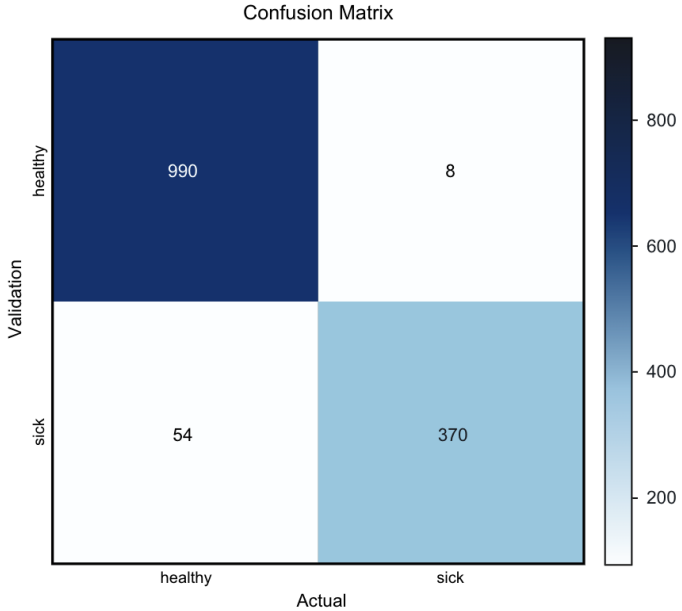

Figure 6. CNN Confusion Matrix

Figure 6 presents the confusion matrix results, which were used to evaluate the performance of the CNN model in predicting and distinguishing between two main categories: healthy oil palm trees and BSR-infected oil palm trees. In principle, the confusion matrix illustrates the relationship between the model's predictions and the ground-truth labels in the test dataset.

3.2 Siamese Convolutional Neural Network

The training process of the Siamese Convolutional Neural Network (SCNN) model was conducted to evaluate its capability in detecting Basal Stem Rot (BSR) disease in oil palm trees using pre-processed image data. The model achieved strong performance with a loss value of 0.1371, MSE of 0.0365, and an overall accuracy of 0.9648. These results demonstrate that the SCNN model effectively distinguishes between healthy and BSR-infected oil palm trees with consistent accuracy.

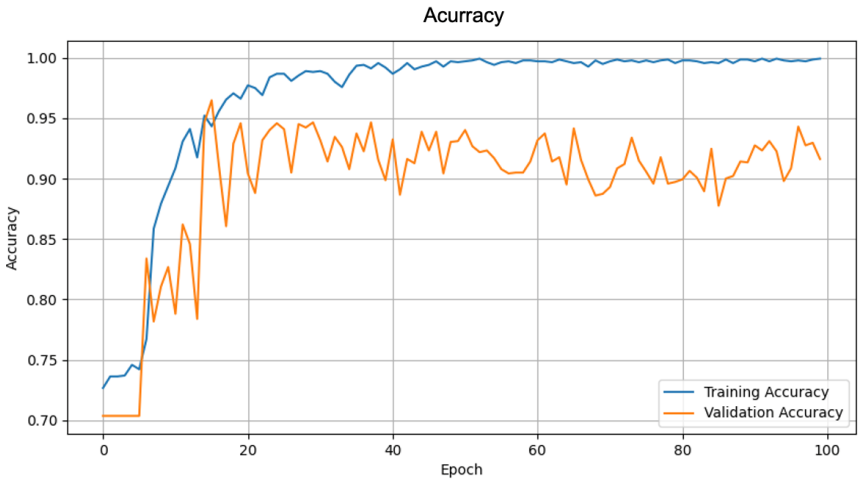

Figure 7. SCNN Acurracy Graph

Figure 7 shows a significant improvement in accuracy during the early phase of training, with rapid performance growth observed up to approximately the 20th epoch. After this point, the training accuracy continued to increase steadily and eventually reached near-perfect stability, while the validation accuracy fluctuated slightly but remained relatively high throughout the training process. This pattern indicates that the SCNN model achieved strong learning performance and was able to generalize effectively to the validation data with minimal overfitting.

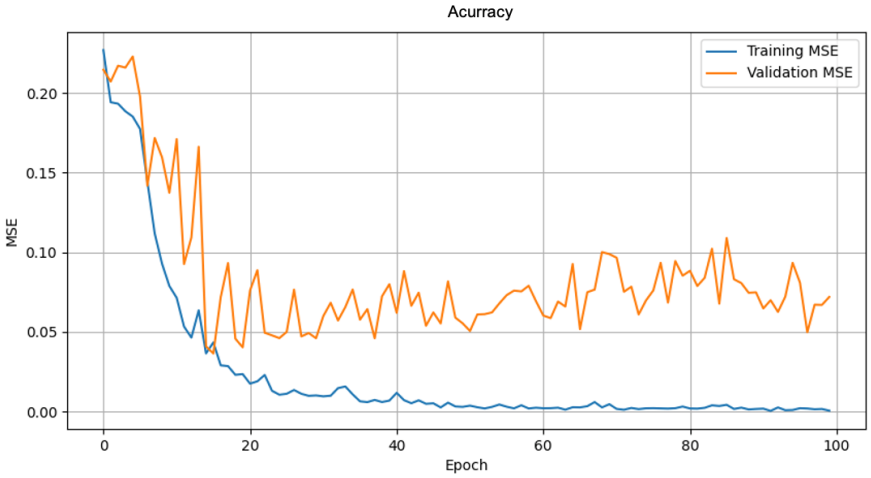

Figure 8. SCNN MSE Graph

Figure 8 shows the MSE curve, which exhibits a substantial decrease during the early stages of training, indicating that the SCNN model rapidly learned to minimize prediction errors. After approximately the 40th epoch, the MSE value stabilized near zero, suggesting that the model reached a convergence point where the difference between predicted and actual values became minimal. Although the validation MSE curve exhibits slight fluctuations, it remains relatively low throughout the training process. This behavior demonstrates that the SCNN model maintains consistent performance and generalizes effectively to previously unseen data. The small gap between the training and validation MSE curves further confirms that the model does not suffer from significant overfitting and performs reliably in predicting image-pair similarities.

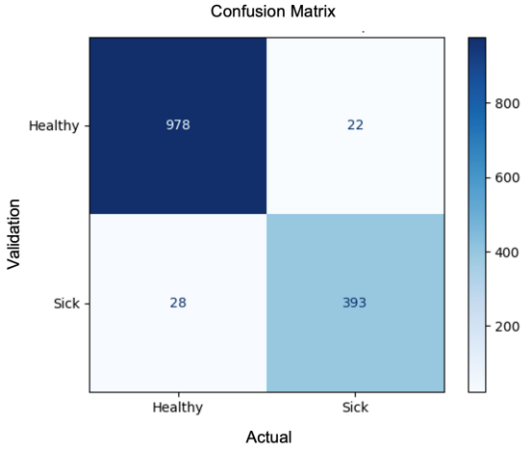

Figure 9. SCNN Confusion Matrix

Figure 9 presents the confusion matrix used to evaluate the performance of the SCNN model across two main categories: healthy and BSR-infected oil palm trees. Based on the matrix, most test samples were correctly classified into their respective categories. The high values of TP and TN indicate that the model demonstrates strong sensitivity and specificity, while the low values of FP and FN indicate that classification errors remain minimal.

3.3 Model Comparison

The performance comparison between the CNN and SCNN was conducted to evaluate the effectiveness of each model in detecting BSR disease in oil palm trees. The evaluation includes several performance metrics, namely accuracy, loss, and MSE. Table 3 presents the comparative results of both models

Table 3. Comparison of Model Evaluation with Previous Studies

Model	Acurracy	MSE	Loss	Precision	Recall	F1-Score
M-CR U-Net[4]	-	-	-	0.989	0.982	0.978
YOLOv5[9], [26]	-	-	-	0.961	0.813	0.787
ANN [26]	0.947	-	0.2158	0.900	0.783	0.837
CNN	**0.9564**	**0.4663**	**0.1876**	**0.8726**	**0.9789**	**0.923**
SCNN	**0.9648**	**0.0365**	**0.1371**	**0.9469**	**0.9334**	**0.9399**

Based on the comparative evaluation presented in Table 3, the SCNN model consistently outperforms other models, including those reported in previous studies such as M-CR U-Net, YOLOv5, and ANN. This superior performance is reflected not only in higher classification accuracy but also in substantially lower prediction errors, as indicated by the MSE and loss values. These findings suggest that the SCNN model is more effective in learning discriminative feature representations while minimizing prediction errors during the training process. Furthermore, the balanced values of precision, recall, and F1-score demonstrate that the SCNN model maintains a strong balance between correctly identifying BSR-infected oil palm trees and minimizing false detections, which is particularly important for early-stage disease detection.

When compared with the standard CNN model, the SCNN shows consistent improvements across all evaluation metrics. Notably, the reduction in error-related metrics indicates enhanced model robustness and improved generalization capability. This improvement is likely attributed to the Siamese architecture, which enables more effective feature comparison and reduces redundancy in feature learning. As a result, the SCNN produces more stable and reliable performance when distinguishing between healthy and BSR-infected oil palm images. Overall, these findings confirm that the proposed SCNN approach provides the most effective performance for detecting BSR symptoms in oli plam trees, outperforming both conventional deep learning models and methods reported in previous studies.

4. Conclusion

This research presents the successful development and evaluation of CNN and SCNN models for identifying BSR disease in oil palm trees. The evaluation results show that the SCNN architecture achieve better performance than the standard CNN model. The SCNN achieved an accuracy of 96.48%, while the CNN acieved an accuracy of 95.64%. These findings indicate that the integration of a Siamese architecture, combined with additional convolutional structures, enhances the model's capability to extract more discriminative features while maintaining balanced performance in

terms of precision and recall. Consequently, the SCNN model exhibits stronger generalization capability and a lower tendency toward overfitting, making it a reliable approach for the early detection of BSR disease in oil palm plantations.

Acknowledgement

The authors would like to express their sincere gratitude to Brawijaya University for providing an academic environment that supported the development of this research. It is hoped that the findings of this study will contribute meaningfully to technological advancements in Indonesia.

References

[1] *2018 International Conference On Signals And Systems : Proceedings : May 1-3, 2018, Prama Sanur Beach Hotel, Bali, Indonesia*. IEEE, 2018.
[2] Y. Siddiqui, A. Surendran, R. R. M. Paterson, A. Ali, And K. Ahmad, "Current Strategies and Perspectives In Detection And Control Of Basal Stem Rot Of Oil Palm," May 01, 2021, *Elsevier B.V.* https://doi.org/10.1016/J.Sjbs.2021.02.016
[3] Y. Xu *Et Al.*, "Author Correction: Recent Expansion Of Oil Palm Plantations Into Carbon-Rich Forests (Nature Sustainability, (2022), 10.1038/S41893-022-00872-1)," May 01, 2022, *Nature Research*. https://doi.org/10.1038/S41893-022-00897-6
[4] O. Win Kent, T. Weng Chun, T. Lee Choo, And L. Weng Kin, "Early Symptom Detection of Basal Stem Rot Disease In Oil Palm Trees Using A Deep Learning Approach On UAV Images," *Comput Electron Agric*, Vol. 213, Oct. 2023. https://doi.org/10.1016/J.Compag.2023.108192
[5] Y. H. Haw *Et Al.*, "Classification Of Basal Stem Rot Using Deep Learning: A Review of Digital Data Collection And Palm Disease Classification Methods," *Peerj Comput Sci*, Vol. 9, 2023. https://doi.org/10.7717/PEERJ-CS.1325
[6] P. Ahmadi, S. Mansor, B. Farjad, And E. Ghaderpour, "Unmanned Aerial Vehicle (UAV)-Based Remote Sensing For Early-Stage Detection Of Ganoderma," *Remote Sens (Basel)*, Vol. 14, No. 5, Mar. 2022. https://doi.org/10.3390/Rs14051239
[7] M. A. Istiak et al., "Adoption of Unmanned Aerial Vehicle (UAV) imagery in agricultural management: A systematic literature review," Dec. 01, 2023, Elsevier B.V. https://doi.org/10.1016/j.ecoinf.2023.102305
[8] M. Lestandy And A. Nugraha, "UAV Image Classification Of Oil Palm Plants Using CNN Ensemble Model," 2025.
[9] Y. Nuwara, W. K. Wong, And F. H. Juwono, "Modern Computer Vision For Oil Palm Tree Health Surveillance Using Yolov5," In *2022 International Conference On Green Energy, Computing And Sustainable Technology, GECOST 2022*, Institute Of Electrical And Electronics Engineers Inc., 2022, Pp. 404–409. https://doi.org/10.1109/GECOST55694.2022.10010668
[10] M. Al-Shalout And K. Mansour, "Detecting Date Palm Diseases Using Convolutional Neural Networks," In *2021 22nd International Arab Conference On Information Technology, ACIT 2021*, Institute Of Electrical And Electronics Engineers Inc., 2021. https://doi.org/10.1109/ACIT53391.2021.9677103
[11] Rahmadwati, A. Zahfran Imran, M. Aswin, And K. Ferdiana, "Identifikasi Penyakit Katarak Berdasarkan Citra Fundus Menggunakan Siamese Convolutional Neural Network". https://doi.org/10.26760/elkomika.v12i4.838
[12] E. Sugiarto, F. Budiman, And A. Fahmi, "Implementation Of Deep Learning Based On Convolution Neural Network For Batik Pattern Recognition," *Kinetik: Game Technology, Information System, Computer Network, Computing, Electronics, And Control*, Jan. 2025. https://doi.org/10.22219/kinetik.v10i1.2019
[13] Y. Zhang, J. Zhang, And W. Zhou, "Research On Image Classification Improvement Based On Convolutional Neural Networks With Mixed Training," In *Proceedings Of 2022 IEEE 4th International Conference On Civil Aviation Safety And Information Technology, ICCASIT 2022*, Institute Of Electrical And Electronics Engineers Inc., 2022, Pp. 7–10. https://doi.org/10.1109/ICCASIT55263.2022.9986643
[14] A. Perdananto, A. Udin Zailani, J. Kencana No, And P. Tangerang Selatan, "Penerapan Deep Learning Pada Aplikasi Prediksi Penyakit Pneumonia Berbasis Convolutional Neural Networks," *DES 2019 Journal Of Informatics And Communications Technology*, Vol. 1, No. 2, Pp. 1–010. https://doi.org/10.52661/j_ict.v1i2.34
[15] H. Hamdani, A. Septiarini, A. Sunyoto, S. Suyanto, And F. Utaminingrum, "Detection Of Oil Palm Leaf Disease Based On Color Histogram And Supervised Classifier," *Optik (Stuttg)*, Vol. 245, Nov. 2021. https://doi.org/10.1016/J.Ijleo.2021.167753
[16] I. Wulandari, H. Yasin, And T. Widiharih, "Klasifikasi Citra Digital Bumbu dan Rempah Dengan Algoritma Convolutional Neural Network (CNN)". https://doi.org/10.14710/j.gauss.9.3.273-282
[17] A. Anhar and R. A. Putra, "Perancangan dan Implementasi Self-Checkout System pada Toko Ritel menggunakan Convolutional Neural Network (CNN)," ELKOMIKA: Jurnal Teknik Energi Elektrik, Teknik Telekomunikasi, & Teknik Elektronika, vol. 11, no. 2, p. 466, Apr. 2023. https://doi.org/10.26760/elkomika.v11i2.466
[18] I. Nasution, A. Perdana Windarto, And M. Fauzan, "Penerapan Algoritma K-Means Dalam Pengelompokan Data Penduduk Miskin Menurut Provinsi," *Technology And Science (BITS*, Vol. 2, No. 2, Pp. 76–83, 2020. https://doi.org/10.47065/bits.v2i2.492
[19] A. A. Nilatika, S. H. Pramono, And Rahmadwati, "Early Diagnosis Of Diabetic Retinopathy Through Optimization Of Convolutional Neural Network Hyperparameters Using Genetic Algorithm," In *ICSINTESA 2024 - 2024 4th International Conference Of Science And Information Technology In Smart Administration: The Collaboration Of Smart Technology And Good Governance For Sustainable Development Goals*, Institute Of Electrical And Electronics Engineers Inc., 2024, Pp. 384–389. https://doi.org/10.1109/ICSINTESA62455.2024.10747887
[20] G. Zhao, L. Xu, X. Zhu, S. Lin, And L. Xie, "Spectrum-Matched Ground Motion Selection Method Based On Siamese Convolutional Neural Networks," *Soil Dynamics And Earthquake Engineering*, Vol. 163, Dec. 2022. https://doi.org/10.1016/J.Soildyn.2022.107515
[21] M. Toby Suwindra, A. Erlansari, And J. W. Supratman Kandang Limun, "Analisis Kemiripan Jenis Burung Menggunakan Siamese Neural Network Analysis of Bird Species Similarity Using Siamese Neural Network," 2021. https://doi.org/10.33369/rekursif.v9i2.18584
[22] J. Sunkpho, C. Se, W. Wipulanusat, And V. Ratanavaraha, "SHAP-Based Convolutional Neural Network Modeling For Intersection Crash Severity On Thailand's Highways," *IATSS Research*, Vol. 49, No. 1, Pp. 27–41, Apr. 2025. https://doi.org/10.1016/J.Iatssr.2024.12.003
[23] P. Narmatha, S. Gupta, T. R. Vijaya Lakshmi, And D. Manikavelan, "Skin Cancer Detection From Dermoscopic Images Using Deep Siamese Domain Adaptation Convolutional Neural Network Optimized With Honey Badger Algorithm," *Biomed Signal Process Control*, Vol. 86, Sep. 2023. https://doi.org/10.1016/J.Bspc.2023.105264
[24] C. Jingying et al., "Rapid and accurate classification of Dioscorea species using Attenuated Total Reflection-Fourier Transform Infrared (ATR-FTIR) spectroscopy integrated with chemometric analysis and Convolutional Neural Network (CNN)," Applied Food Research, p. 102213, May 2026. https://doi.org/10.1016/j.afres.2026.102213
[25] M. Dandi Darojat, Y. A. Sari, and R. C. Wihandika, "Convolutional Neural Network untuk Klasifikasi Citra Makanan Khas Indonesia," 2021.
[26] P. Mimboro, B. Soewito, H. Soeparno, And W. Budiharto, "Prediction Of Oil Palm Conditions Using Deep Learning Based On The Visible Atmospherically Resistant Index On UAV Imagery," In *INCITEST 2023 - Proceedings Of The 2023 International Conference On Informatics Engineering, Science And Technology*, Institute Of Electrical And Electronics Engineers Inc., 2023. https://doi.org/10.1109/INCITEST59455.2023.10396901